



Design and characterization of chimeric Rabies-SARS-CoV-2 virus-like particles for vaccine purposes

Ernesto Garay¹ · Diego Fontana¹ · Javier Villarraza¹ · Antonela Fuselli¹ · Agustina Gugliotta¹ · Sebastián Antuña² · Belén Tardivo² · María Celeste Rodríguez¹ · Victoria Gastaldi^{1,2} · Juan Manuel Battagliotti¹ · Diego Alvarez³ · Eliana Castro³ · Juliana Cassataro³ · Natalia Ceaglio¹ · Claudio Prieto^{4,2,5}

Received: 2 December 2022 / Revised: 16 March 2023 / Accepted: 17 April 2023 / Published online: 1 May 2023
© The Author(s), under exclusive licence to Springer-Verlag GmbH Germany, part of Springer Nature 2023

Abstract

Due to the high number of doses required to achieve adequate coverage in the context of COVID-19 pandemics, there is a great need for novel vaccine developments. In this field, there have been research approaches that focused on the production of SARS-CoV-2 virus-like particles. These are promising vaccine candidates as their structure is similar to that of native virions but they lack the genome, constituting a biosafe alternative. In order to produce these structures using mammal cells, it has been established that all four structural proteins must be expressed. Here we report the generation and characterization of a novel chimeric virus-like particle (VLP) that can be produced by the expression of a single novel fusion protein that contains SARS-CoV-2 spike (S) ectodomain fused to rabies glycoprotein membrane anchoring region in HEK293 cells. This protein is structurally similar to native S and can autonomously bud forming enveloped VLPs that resemble native virions both in size and in morphology, displaying S ectodomain and receptor binding domain (RBD) on their surface. As a proof of concept, we analyzed the immunogenicity of this vaccine candidate in mice and confirmed the generation of anti-S, anti-RBD, and neutralizing antibodies.

Key points

- A novel fusion rabies glycoprotein containing S ectodomain was designed.
- Fusion protein formed cVLPs that were morphologically similar to SARS-CoV-2 virions.
- cVLPs induced anti-S, anti-RBD, and neutralizing antibodies in mice.

Keywords Spike · Chimeric · VLP · RBD · Rabies

✉ Diego Fontana
dfontana@fbc.unl.edu.ar

¹ UNL, CONICET, FBCB (School of Biochemistry and Biological Sciences), CBL (Biotechnological Center of Litoral), Ciudad Universitaria, Ruta Nacional 168 - Km 472.4 - C.C. 242 - (S3000ZAA) Santa Fe, Santa Fe, Argentina

² Biotecnofe S.A. PTLC, Ruta 168 (S3000ZAA) Santa Fe, Santa Fe, Argentina

³ Instituto de Investigaciones Biotecnológicas “Dr. Rodolfo A. Ugalde” UNSAM-CONICET, Pcia. Buenos Aires, San Martín, Argentina

⁴ UNL, FBCB (School of Biochemistry and Biological Sciences), CBL (Biotechnological Center of Litoral), Ciudad Universitaria, Ruta Nacional 168 - Km 472.4 - C.C. 242 - (S3000ZAA) Santa Fe, Santa Fe, Argentina

⁵ Cellargen Biotech SRL, FBCB (School of Biochemistry and Biological Sciences) Biotechnological Development Laboratory, Ciudad Universitaria UNL, (S3000ZAA) Santa Fe, Argentina

Introduction

Coronavirus disease 2019 (COVID-19) pandemic has impacted enormously on society both in health and in economic aspects, causing more than 6 million human deaths and over 759 million cases all over the world since its beginning (<https://covid19.who.int/>). Its highly contagious nature has challenged the public health services and caused multimillionaire loses due to measures imposed to restrict viral circulation (Cutler and Summers 2020). It is caused by a betacoronavirus named *severe acute respiratory syndrome coronavirus 2* (SARS-CoV-2), an enveloped virus containing a single positive stranded RNA genome and four structural proteins: nucleocapsid protein (N), membrane protein (M), envelope protein (E), and spike glycoprotein (S). The last one is responsible for virus entry into cells by interacting with angiotensin converting enzyme 2 (ACE2) through the receptor binding domain (RBD) (Tai et al. 2020). Once the virus is attached, a serin protease cleaves S allowing it to undergo a conformational change that triggers host cell and viral membrane fusion (Walls et al. 2020).

Since S glycoprotein has a key role during infection, it has been the main target for vaccine development with good results, either as a coding sequence that the vaccinated individual will express in vivo (in the case of mRNA and adenoviral vectors) (Polack et al. 2020; Voysey et al. 2021; Baden et al. 2021; Sadoff et al. 2021), or directly incorporated in the formulation in the context of an inactivated virus or as a recombinant antigen (Xia et al. 2021; Tanriover et al. 2021; Heath et al. 2021). There is another type of recombinant antigen vaccine technology that mimics the structure of the viral particle but does not contain the viral genome, so it is biosafe. These structures called virus-like particles (VLPs) are able to trigger potent immune responses due to their particulate and multivalent nature (Lua et al. 2014; Donaldson et al. 2018), and have been applied successfully for hepatitis B virus and human papilloma virus (Schiller et al. 2012; Etzion et al. 2016). In the case of COVID-19, the first VLP-based vaccine was approved recently in Canada (Covifenz, (Hager et al. 2022)). The immunogen consists in a full-length S protein embedded on a lipidic membrane, which is recombinantly expressed in tobacco plants. It has shown good immunogenic properties in combination with an oil-in-water adjuvant (Garçon et al. 2012), despite the fact that plant glycosylation patterns are very different to mammalian ones. There have also been attempts to produce SARS-CoV-2 VLPs using mammalian cells, but it has been demonstrated that the other structural proteins of SARS-CoV-2 (M, N, and E) must be co-expressed with S in order to obtain particles (Xu et al. 2020; Swann et al. 2020).

Besides, VLPs can also be modified to display heterologous domains or epitopes on their surface by fusing them to the viral proteins that constitute the VLP. These chimeric VLPs (cVLPs) can induce potent immune responses

against the foreign inserted sequences, and can be a viable alternative for viruses that do not easily form VLPs or for other types of microorganisms such as parasites (Xu et al. 2015; del Carmen et al., 2016; Mareze et al. 2016; Liu et al. 2017; Aston-Deaville et al. 2020; Czarnota et al. 2020). In fact, there is an approved malaria vaccine based on this technology (Laurens 2020). In our laboratory, we have developed, characterized, and licensed a novel highly immunogenic rabies VLP that is produced by expression of rabies glycoprotein (RVG) in HEK293 cells, which buds forming enveloped particles (Fontana et al. 2014; Fontana et al. 2015b; Fontana et al. 2016; Fontana et al. 2019; Fontana et al. 2020). This fact has also been reported by other research groups, which could detect RVG in “shed” particles (Callaway et al. 2022). In previous experiments, we were able to confirm RVG VLP ability to expose heterologous epitopes on their surface, by fusing a neutralizing epitope of foot-and-mouth disease virus with different regions of RVG (Fontana et al. 2021b; Garay et al. 2022). In this work, we aimed to take advantage of the autonomous budding activity and heterologous display ability of RVG to generate a novel cVLP that exposes S on its surface for vaccine purposes, as an alternative to the autologous SARS-CoV-2 VLPs that require co-expression of N, M, and E proteins. A novel fusion S-RVG protein was designed, and its expression and plasma membrane localization was studied. cVLPs were morphologically characterized and their immunogenicity was confirmed in mice, detecting both anti-S and neutralizing antibodies.

Materials and methods

Sequence design and molecular cloning

Sequences of S (Wuhan, GenBank accession no MN908947.3), RVG (Pasteur strain, GenBank accession no AAA47218.1), and CD33 signal peptide (GenBank accession no BC028152.1) were obtained from the National Center for Biotechnology Information database. The coding sequence for S-RVG chimeric construction (GenBank accession no OP912878) (encompassing AA 1-17 of CD33 protein, AA 16-1212 of S and AA 389-505 of RVG) was chemically synthesized and cloned into a third-generation lentiviral transference vector (Prieto et al. 2011) (pLV-S-RVG) under the influence of a human elongation factor 1 α promoter. This construct was verified by Sanger sequencing.

SARS-CoV-2 virus-like particle expression and purification

VLPs were expressed in HEK293 cells by transient transfection and concentrated by ultracentrifugation. Twenty-four

hours prior to transfection cells were seeded at a density of 4×10^5 cells ml^{-1} in 175 cm^2 T flasks and incubated overnight (ON) at 37°C and $5\% \text{ CO}_2$. The transfection was performed using $5 \mu\text{g}$ of DNA per 10^6 cells and PEI/DNA polyplexes were formed by adding PEI to plasmid DNA (in a 1.5:1 ratio) diluted in DMEM. Complexes were incubated for 15 min at room temperature (RT) and added to the culture. Four hours post-transfection (hpt), cell supernatant was removed and replaced by fresh complete medium containing valproic acid (1.68 mM) and caffeine (2.5 mM) (Sigma-Aldrich).

Seventy-two hpt cell supernatant containing VLPs was harvested and clarified by centrifugation at $4000 g$ for 20 min. The clarified supernatant was layered over a 30% sucrose cushion and centrifuged at $60,000 g$ for 5 h at 4°C (Beckman JA-20 rotor, Beckman Avanti J-E, Beckman Coulter). VLP pellet was resuspended in PBS using 1% of the original volume and stored at 4°C .

Chimeric protein expression analysis by flow cytometry and laser confocal microscopy

HEK293 cells were transfected with pLV-S-RVG and protein expression was analyzed 72 hpt. Twenty-four hours prior to transfection, cells were seeded at a density of 2×10^5 cells ml^{-1} in 12-well plates and incubated ON at 37°C and $5\% \text{ CO}_2$. The transfection was performed using $1 \mu\text{g}$ of DNA per 10^6 cells, using Lipofectamine® 3000 (ThermoFisher Scientific) as transfection reagent in a 2:1 Lipid:DNA relation. Complexes were incubated for 20 min at RT and then added to the culture. Four hpt, the DNA/lipid mixture was removed and replaced by fresh complete medium containing valproic acid (1.68 mM) and caffeine (2.5 mM). Seventy-two hpt, cells were trypsinized and washed with PBS, and then they were incubated with either an anti-SARS-CoV-2 RBD monoclonal antibody (mAb) (NN68, Creative Diagnostics) diluted 1/500 in PBS, or a convalescent serum diluted 1/200 in PBS for 45 min at RT. NN68 mAb is a neutralizing SARS-CoV-2 antibody, with a IC_{50} of $0.41 \mu\text{g mL}^{-1}$, as measured by the *in vitro* pseudovirus neutralization assay. After another wash with PBS, cells were incubated with either a goat anti-mouse antibody or a goat anti-human antibody conjugated to AlexaFluor488 (ThermoFisher Scientific), both diluted 1/500 in PBS, for 30 min at RT. A final wash was performed, and cells were resuspended in $200 \mu\text{l}$ of PBS and analyzed in a GUAVA EasyCyte cytometer (Millipore) using Guava Express Plus Software (Millipore).

To analyze the localization of S-RVG on plasma membrane, a laser confocal microscopy was performed. Immunostained transfected cells were incubated for 15 min at RT with a solution containing Hoechst $1 \mu\text{g mL}^{-1}$ (ThermoFisher Scientific) and orange Cytopainter cell plasma membrane staining kit

diluted 1:500 (Abcam) in PBS for nuclei and plasma membrane staining, respectively. Then, cells were washed, resuspended in PBS, and observed in a Leica-TCS-SP8 confocal microscope (Leica). Images were analyzed using ImageJ software (Schindelin et al. 2012).

Western blot

VLP samples and culture supernatants were mixed with $4\times$ sample buffer (2% SDS, 10% glycerol, 50 mM Tris-HCl pH, 6.8, 0.05% bromophenol blue) and boiled for 5 min. After that, samples were separated by 10% SDS-PAGE and proteins were transferred to a PVDF membrane (Bio-Rad Laboratories) and blocked with TBS, 5% skim milk (50 mM Tris-HCl, pH 7.5, 150 mM NaCl). Proteins were detected with an anti-SARS-CoV-2 RBD mAb (NN68) diluted 1/1000 in TBS, 0.5% skim milk, and 0.05% Tween 20, and a HRP-conjugated goat anti-mouse secondary antibody (Dako, Agilent Technologies) diluted 1/700 in TBS, 0.5% skim milk, and 0.05% Tween 20. The reaction was revealed using a chemiluminescent reagent (Pierce™ ECL Western Blotting substrate, Thermo Fisher Scientific).

Electron microscopy analysis of SARS-CoV-2 VLPs

VLP morphology was analyzed by transmission electron microscopy (TEM). Briefly, $10 \mu\text{l}$ of VLP preparation was adsorbed onto Formvar-coated 200-mesh copper grids (Ted Pella, Inc.) for 2 min and then negatively stained with 2% uranyl acetate for 2 min. Samples were observed in a transmission electron microscope (JEM-2100 plus, Jeol).

For gold-immunolabeling, after VLP adsorption, the grids were blocked with PBS-BSA 1% for 30 min and then incubated for 60 min with an anti-SARS-CoV-2 RBD mAb (NN68) diluted 1/20 dilution in PBS-BSA 0.05%. After a washing step, the grid was incubated with a secondary 10-nm gold-conjugated anti-mouse IgG antibody (G7777, Sigma-Aldrich) diluted 1/20 in PBS-BSA 1% for 60 min. A final wash was performed, and the grids were negatively stained with 2% uranyl acetate for 2 min before TEM observation. All incubations were done in a humid chamber. Electron micrographs were analyzed and cVLP size was measured using ImageJ software (Schindelin et al. 2012).

Pseudotyped lentivirus production and ACE2 transduction assay

An established protocol for pseudotyped lentivirus production was followed (Crawford et al. 2020). Briefly, HEK293T cells were co-transfected using PEI with the plasmids HDM-Hgpm2, HDM-tat1b, pRC-CMV-Rev1b, and pHAGE2-CMV-ZsGreen-W, and a plasmid encoding the envelope protein, i.e., HDM-IDTSpike-fix, for wt S

protein or pLV-S-RVG for the fusion protein pseudotype. As a negative control, a lentiviral stock without any envelope protein was constructed. Forty-eight hours post transfection, supernatants were collected and clarified at 4000 *g* for 20 min, and then concentrated by ultracentrifugation at 60,000 *g* for 5 h at 4 °C (Beckman JA-20 rotor, Beckman Avanti J-E, Beckman Coulter). Pellets were resuspended in DMEM with 3% of the original volume and stored at –70 °C.

HEK293 cells expressing ACE2 were used to analyze S-RVG ability to interact with ACE2 receptor and mediate lentiviral transduction. For this, HEK293-ACE2 or wt HEK293 cells were plated on 96-well plates at 3.5×10^4 cells ml^{-1} 24 h prior to the transduction experiment. Then, culture supernatants were removed and concentrated lentivirus samples diluted 1:2 in DMEM complete medium were added over the cells by triplicate. Seventy-two hours later, ZsGreen expression on transduced cells was measured by flow cytometry with a GUAVA EasyCyte cytometer using Guava Express Plus Software.

Fluorescent S-RVG cVLP production and ACE2 binding assay

Fluorescent S-RVG cVLPs were obtained by co-expression of S-RVG with Gag-GFP fluorescent fusion protein by transient transfection of HEK293 cells, and concentrated by ultracentrifugation. Twenty-four hours prior to transfection, cells were seeded at a density of 4×10^5 cells ml^{-1} in 175 cm^2 T flasks and incubated ON at 37 °C and 5% CO_2 . The transfection was performed using 2.5 μg of pLV-S-RVG and 2.5 μg of pGag-EGFP (Cervera et al. 2013) per 10^6 cells. PEI/DNA polyplexes were formed by adding PEI to plasmid DNA diluted in DMEM in a 1.5:1 ratio. Complexes were incubated for 15 min at RT and added to the culture. Four hpt, cell supernatant was removed and replaced by fresh complete medium containing valproic acid (1.68 mM) and caffeine (2.5 mM). Particles containing only Gag-GFP were obtained by transfection of 5 μg of pGag-EGFP per 10^6 cells, following the same protocol. Seventy-two-hpt cell supernatant containing VLPs was harvested and clarified by centrifugation at 4000 *g* for 20 min. The clarified supernatant was layered over a 30% sucrose cushion and centrifuged for 5 h at 4 °C (Beckman JA-20 rotor, Beckman Avanti J-E). VLP pellet was resuspended in PBS with 1% of the original volume and maintained at 4 °C. Concentrated fluorescent VLPs were quantified by fluorimetry using a microplate fluorimeter (Thermo Scientific Fluoroskan FL, ThermoFisher Scientific).

To analyze if fluorescent cVLPs were able to interact with ACE2, a binding assay was performed on HEK293-ACE2 cells. Twenty-four hours prior to the binding assay, ACE2 and wt HEK293 cells were plated on 96-well plates at a

density of 2×10^4 cells per well in 200 μl and incubated ON at 37 °C and 5% CO_2 . The next day, concentrated fluorescent VLPs were diluted with DMEM complete medium, in order to normalize the number of fluorescent particles previously quantified by fluorimetry, and incubated on the plated cells in triplicate for 2 h at 37 °C and 5% CO_2 . Finally, supernatant was removed, and the percentage of fluorescent cells was measured by flow cytometry with a GUAVA EasyCyte cytometer using Guava Express Plus Software.

Mice immunization

The immunization protocols were approved and supervised by the Advisory Committee on Ethics and Security of the School of Biochemistry and Biological Sciences, Universidad Nacional del Litoral, according to international guidelines (“Guide for the Care and Use of Laboratory Animals,” Eighth Edition, National Research Council 2011). Female Balb/c mice of 6–8 weeks of age (SPF, Centro de Medicina Comparada, ICIVET- CONICET-UNL, Argentina) were intramuscularly immunized at days 0 and 21.

Animals vaccinated with VLPs ($n=7$) received a dose of 150 ng, considering only the chimeric S-RVG protein content. VLPs were formulated with LipoSap® adjuvant in a final concentration of 100 μg ml^{-1} . This is a commercial presentation of the adjuvant called ISPA (Bertona et al. 2017), which consists of cage-like particles with low surface charge density containing Quil-A® as immune response stimulator, and it was obtained from Lipomize S.R.L., Argentina. LipoSap® adjuvant was previously tested for other vaccine candidates for hepatitis B, rabies, and foot-and-mouth disease (Battagliotti et al. 2020; Bidart et al. 2020; Fontana et al. 2020; Bidart et al. 2021; Fontana et al. 2021b).

Fifteen days after second dose, mice bled and sera collected and conserved at –20 °C for analysis. Pre-immune sera also were collected before starting the immunization.

On days 114 and 148 from priming, mice serum samples were obtained again for antibody titer analysis. Further, on day 155 from priming, mice were injected with a booster containing the same amount of antigen of the previous doses and on the 171 (16 days after boosting) serum samples were obtained.

ELISA for anti-S or anti-RBD antibody detection

Plates were coated with 150 ng per well of purified RBD or S protein and incubated ON at 4 °C. Plates were washed six times with PBS-Tween-20 0.05% and then blocked with 200 μl per well of 2% skim milk in PBS for 1 h at 37 °C. Twofold serial dilutions of sera samples in skim milk 0.2%, PBS-Tween-20 0.05% were incubated for 1 h at 37 °C. After that, 100 μl of an HRP-conjugated anti-mouse

antibody (Invitrogen) diluted 1:700 in skim milk 0.2%, and PBS-tween-20 0.05% was added to each well and incubated for 1 h at 37 °C. Six washes with PBS-Tween–20 0.05% were done between each incubation. Finally, the reaction was revealed by adding 100 µl of a chromogenic substrate solution to each well (0.5 mg ml⁻¹ o-phenylenediamine (Sigma-Aldrich), 0.5 µl ml⁻¹ H₂O₂ 30 vol., 50 mM citrate/phosphate buffer, pH 5.3). The reaction was stopped by adding 50 µl of a 0.5 M H₂SO₄ solution and the optical density was measured at 492 nm in a plate reader spectrophotometer (Labsystems Multiskan®). Antibody titers were calculated as the end-point serum dilution yielding an optical density higher than the cutoff value. This cutoff was calculated as the mean + 2 SD of the optical density of negative controls (pre-immune mice sera).

Neutralizing antibody assay

Plasma samples were analyzed following a protocol previously described (Coria et al. 2022). Briefly, plasma samples were serially diluted in DMEM 2% FBS starting from a 1:16 dilution, and preincubated with SARS-CoV-2 (ancestral variant) for 1 h at 37 °C. Then, mixture samples were added to VERO cell monolayers using a multiplicity of infection of 0.004 and incubated for 1 h at 37 °C. Afterwards, supernatant containing virus was removed and DMEM 2% FBS was added. Cells were incubated for 72 h at 37 °C in a 5% CO₂ atmosphere. Finally, cells were fixed with paraformaldehyde 4% for 20 min at 4 °C and stained with a methanol-crystal violet solution. The presence of plaques in the monolayer was assessed visually under a microscope. Neutralizing antibody titer was calculated as the higher plasma dilution showing no cytopathic effect

(CPE) in two or three replicate wells. CPE was established as the presence of one or two plaques per well.

Results

Design of a novel RVG fusion protein displaying S domains

S ectodomain region (AA 16–1212) was fused to 389–505 AA from mature RVG (Fig. 1), aiming to preserve RVG localization and budding properties, while exposing the important antigenic regions of S on the surface. This region of RVG encompasses 51 AA of its ectodomain, as it is important for correct protein localization (Larson et al. 2006), and the transmembrane and cytoplasmic regions. Signal peptide was included immediately before of fusion protein coding sequence in order to direct protein expression to the exportation pathway. Besides, S ectodomain sequence included pre-fusion stabilizing mutations: polybasic furin cleavage site was mutated and two consecutive prolines were added (K986P, V987P) (Walls et al. 2020). The entire construct, named S-RVG, has a length of 1333 AA.

Fusion protein expression and plasma membrane localization

In order to characterize S-RVG expression, HEK293 cells were transfected and protein expression was analyzed by flow cytometry (Fig. 2). Cells were immunostained using an anti-RBD monoclonal neutralizing antibody or a convalescent patient serum. S-RVG was correctly

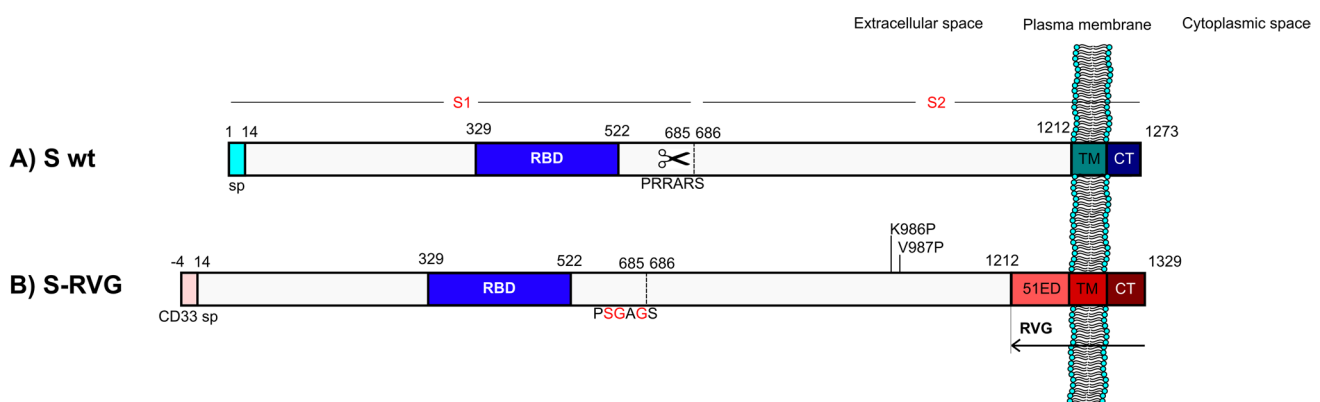


Fig. 1 Schematic representation of chimeric protein in comparison to native S protein. **(A)** Native SARS-CoV-2 S sequence containing a signal peptide (AA 1–15), RBD domain (AA 329–522), a furin cleavage site (AA 685–686) between S1 and S2 domains, and transmembrane (TM) and cytoplasmic (CT) domains. **(B)** Chimeric S-RVG sequence that contains S ectodomain fused to the C-terminal region

of RVG. Signal peptide of CD33 (18 AA) was included before the ectodomain of S, while furin cleavage site was mutated to stabilize the structure. Two consecutive prolines were included on S2 (K986P, V987P) to stabilize the native pre-fusion conformation. After S ectodomain, RVG sequence containing 51 AA of its ectodomain (51ED) and its transmembrane and cytoplasmic domains was inserted.

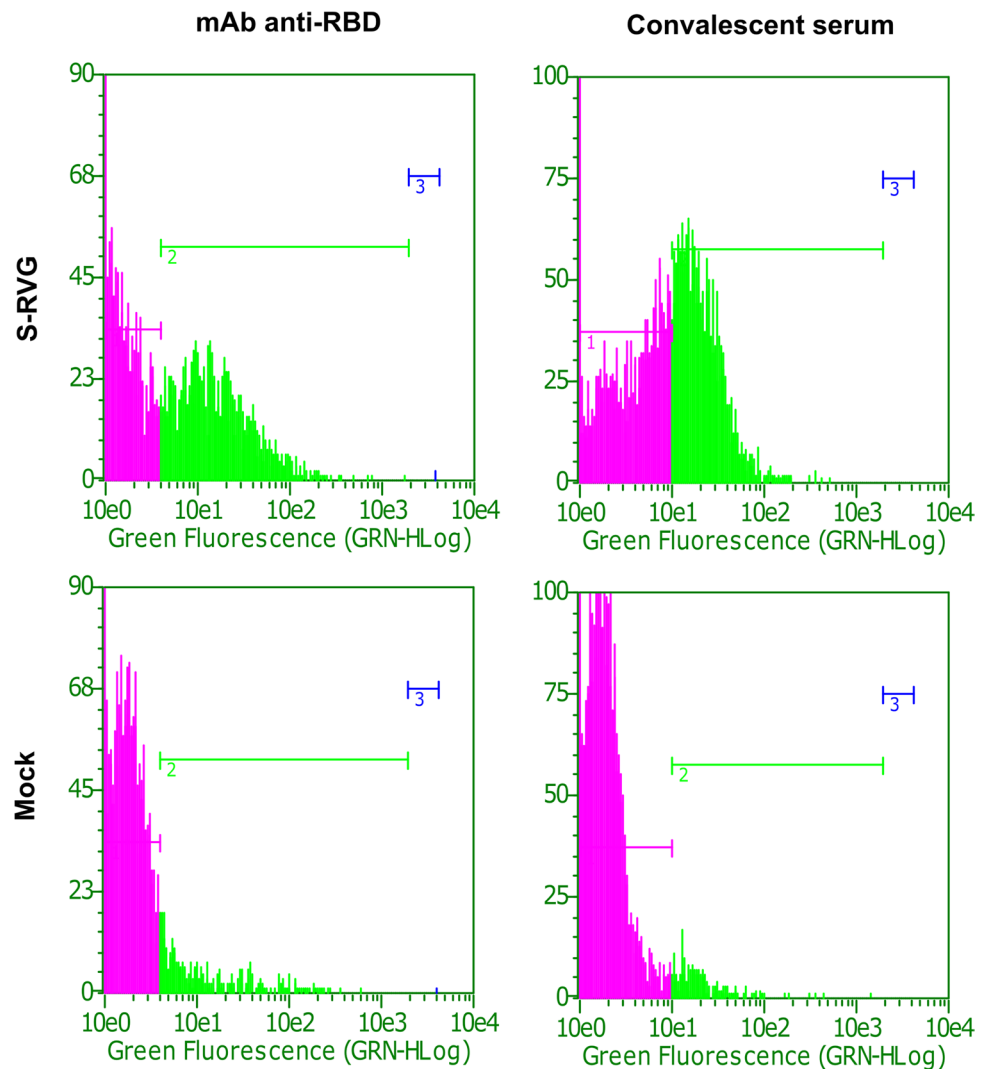
expressed on plasma membrane of expressing cells with an adequate conformation, since it was recognized by both anti-SARS-CoV-2 antibody samples. Importantly, RBD recognition by a neutralizing mAb indicated a proper exposition of this domain on the surface of the protein. In addition, to confirm plasma membrane localization, the same immunostaining procedure was performed and live expressing cells were visualized by laser confocal microscopy (Fig. 3). The fluorescent antibody signals co-localized with that of the plasma membrane staining agent, confirming plasma membrane localization and RBD domain exposure. These results agree with previous publications that described budding of chimeric rabies VLPs from outer cell membrane, with or without other structural viral proteins (Fontana et al. 2019; Fontana et al. 2021a; Garay et al. 2022).

cVLP formation assessment and characterization

Once it was confirmed that S-RVG correctly localized on plasma membrane, its ability to bud forming cVLPs was

evaluated. For this, HEK293 cells were transfected and, after 72 h, culture supernatant was harvested, clarified, and subjected to sucrose cushion ultracentrifugation. Both the culture supernatant and the sucrose cushion sample were analyzed to detect S-RVG by an anti-RBD western blot (Fig. 4). In this way, the presence of full-length S-RVG in both samples, with an approximate molecular weight of 200 KDa, was confirmed, indicating that protein was being released to culture supernatant. However, since the quimera was detected at the bottom of the sucrose cushion, we hypothesized that it was probably associated to a cVLP. To confirm this, this sample was analyzed by TEM (Fig. 5A). Round-shaped particles with an average size of 76 ± 21 nm were observed (Fig. 5C), surrounded by a protein layer that resembled the morphology of SARS-CoV-2 S virions. To confirm that these particles contained S-RVG on their surface, a gold immunolabeled TEM was performed, using a monoclonal anti-RBD antibody and a secondary antibody conjugated to colloidal gold. The high concentration of

Fig. 2 Chimeric protein expression analysis by flow cytometry. HEK293 cells were transfected with pLV-S-RVG or empty pLV plasmid (mock), and 72 hpt cells were immunostained with an anti-RBD mAb or with a convalescent serum, using secondary antibodies conjugated to AlexaFluor488. Marker 1, negative cells. Marker 2 and 3, positive cells



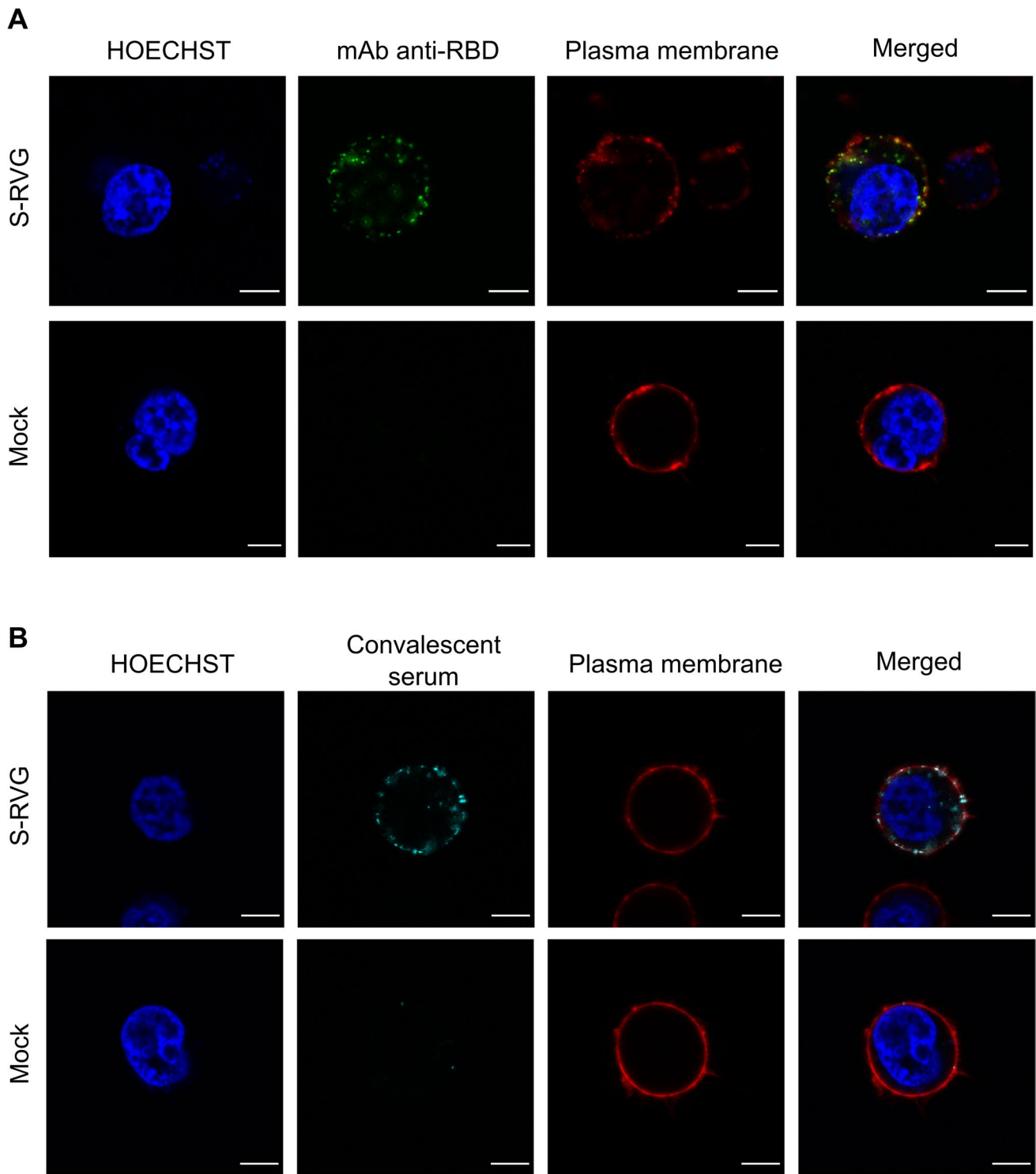


Fig. 3 Plasma membrane localization analysis of the chimeric protein by laser confocal immunofluorescence. HEK293 cells were transfected with pLV-S-RVG or empty pLV plasmid (mock), and 72 hpt cells were immunostained with an anti-RBD mAb (**A**) or with a con-

valent serum (**B**), using secondary antibodies conjugated to AlexaFluor488. Nuclei were stained with Hoechst and plasma membrane with CytoPainter Orange. Scale bar: 6 μ m

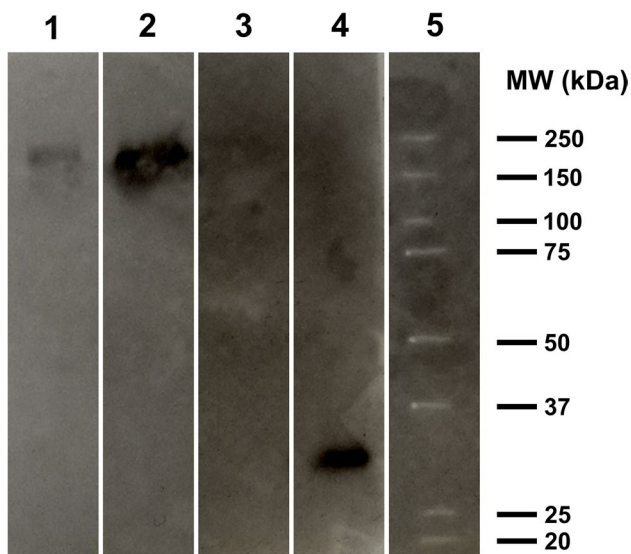


Fig. 4 cVLP detection by western blot. Seventy-two-hour culture supernatants of pLV-S-RVG transfected HEK cells were ultracentrifugated with a sucrose cushion and then analyzed by western blot using an anti-RBD mAb. (1) cVLP ultracentrifugated with a sucrose cushion. (2) cVLPs in the transfection culture supernatant. (3) Mock transfected culture supernatant. (4) Purified RBD. (5) Precision Plus All Blue molecular weight marker (Bio-Rad)

colloidal gold on the surface of the particles (Fig. 5B) confirmed that S-RVG was part of the VLP structure and was anchored on the VLP envelope, and, more importantly, RBD was able to be recognized on the VLP surface by neutralizing antibodies. This result also suggests that RBD adopted an adequate conformation.

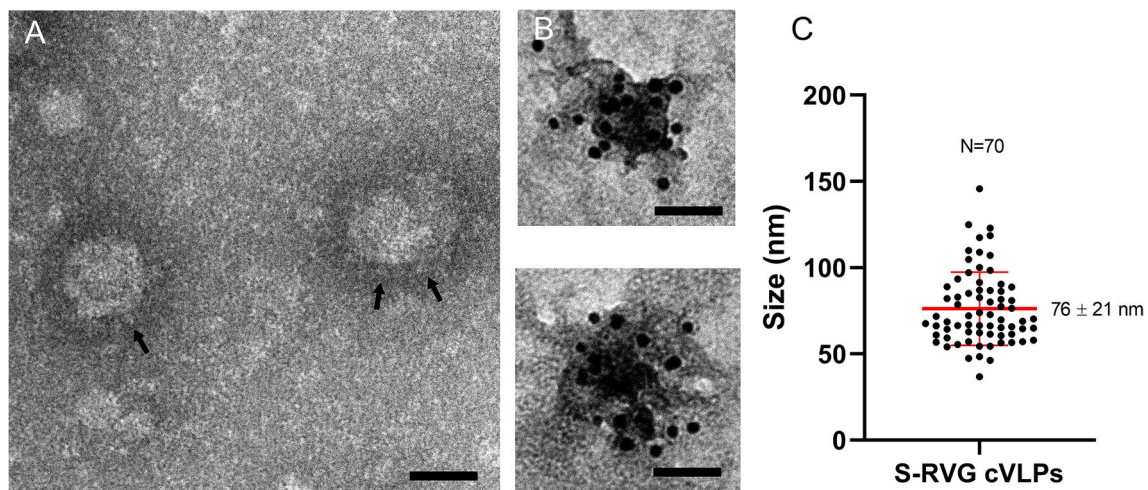


Fig. 5 Transmission electron micrographs of cVLPs. Sucrose cushion purified cVLPs were adsorbed on formvar/carbon coated grids and observed by negative staining (A) or incubated with an anti-RBD mAb and a secondary antibody conjugated to colloidal gold (B).

S-RVG interacts with ACE2 and mediates membrane fusion

To analyze the structure and functionality of the fusion protein, S-RVG pseudotyped lentiviral vectors encoding a fluorescent protein were generated and used to test if this glycoprotein was able to interact with natural SARS-CoV-2 receptor ACE2, triggering plasma membrane fusion to release the lentiviral genome. For this purpose, concentrated pseudotyped lentivirus were added on ACE2-HEK293 cells and the fluorescent protein expression was analyzed by flow cytometry 72 h later (Fig. 6(A)). S-RVG was able to mediate lentiviral transduction at a similar level as wt S protein in a receptor-specific manner, since HEK293 not expressing the receptor were not transduced. This experiment confirmed that the fusion protein structure allows the conformational changes required to mediate membrane fusion, indicating structural similarities to the native S protein.

Furthermore, to analyze if S-RVG was able to interact with ACE2 in the context of cVLPs, fluorescent-labeled cVLPs were generated by co-expression of Gag-GFP reporter protein (Cervera et al. 2013; Gutiérrez-Granados et al. 2013; Fontana et al. 2021b) along with S-RVG. These cVLPs were then incubated with wt or ACE2-expressing HEK293 cells. As a control, Gag-GFP particles without any envelope protein were generated and included in the assay, in order to normalize the content of fluorescent particles and S-RVG-containing cVLPs by fluorimetry. Flow cytometry assays confirmed that fluorescent-labeled S-RVG-cVLPs were able to specifically bind to ACE2 (Fig. 6(B)). This demonstrated that S-RVG adopts an adequate conformation on the surface of cVLPs.

Scale bar: 50 nm. Black arrows indicate S-RVG glycoprotein projections. (C) Size distribution of cVLPs. Error bar in red indicates mean \pm SD

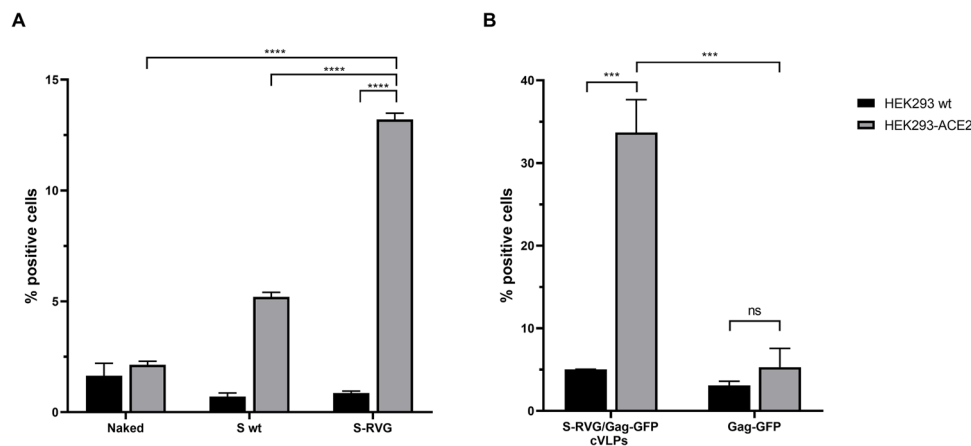


Fig. 6 S-RVG interaction with ACE2 receptor. **(A)** Pseudotyped lentivirus transduction assay on ACE2 expressing cells. ZsGreen encoding lentivirus pseudotyped with wt S protein, S-RVG, or without any envelope protein (naked) were incubated with wt or ACE2 expressing HEK293 cells for 72 h. Percentage of transduced cells was measured by flow cytometry. **(B)** Fluorescent-labeled cVLPs binding to ACE2 expressing cells. Gag-GFP-containing S-RVG cVLPs were generated

and incubated with wt or ACE2 expressing HEK293 cells, revealing the percentage of positive cells by flow cytometry. As a negative control, gag-GFP-containing particles were also generated and included in the assay, normalizing the number of particles by fluorimetry. Bars indicate mean + SD. Tukey multiple comparison test: *** $p < 0.001$, **** $p < 0.0001$, ns: no statistical difference

cVLP immunogenicity

Finally, to test cVLP immunogenicity, an immunization plan was designed. The plan was based on the vaccination of mice with two doses separated by 2 weeks, and a booster delivery 4 months after priming. cVLPs were formulated with ISPA adjuvant (commercially available as LipoSap) which consists of cage-like particles with low surface charge density containing saponin as immune response stimulator (Bertona et al. 2017; Bidart et al. 2020).

The formulation was able to induce S and RBD-specific antibodies after two doses, despite the relatively low amount of antigen inoculated per dose (150 ng of S-containing cVLPs) (Fig. 7A, B). S and RBD-specific antibodies were detected for at least 150 days, and the subsequent booster induced an increment that exceeded the initial antibody levels obtained after two doses. The neutralizing capacity of this antibodies was assessed by analyzing serum samples using a neutralization assay with live virus and VERO cells. Specific neutralizing antibodies could be detected (Fig. 7C), proving that the immunogen has the potential to induce a protective response, although the antigen dose needs to be optimized to further improve antibody levels.

Discussion

The rapid development of vaccines against COVID-19 has been essential to reduce the impact of the disease, with an estimate of 14 million lives saved within the first year of the pandemic (Watson et al. 2022). However, due to the

tremendous amounts of doses required to assure adequate vaccination coverages and booster doses around the world, it is necessary to continue developing new vaccine platforms that can fulfill these demands.

In the field of new-generation vaccines, VLPs have a great potential due to their versatility and immunological properties (Mohsen et al. 2017). In this work, we evaluated a new method to obtain SARS-CoV-2 VLPs containing S protein on their surface for vaccination purposes. Following this objective, we engineered a novel RVG fusion protein to display S ectodomain in order to take advantage of the autonomous budding activity of RVG when overexpressed in HEK293 cells (Fontana et al. 2014; Fontana et al. 2015a).

The designed construct comprises the S protein ectodomain fused to the RVG stem ectodomain region and the transmembrane and cytoplasmic domains (S-RVG) (Fig. 1). This stem, that consists of approximately 50 AA, connects the RVG ectodomain to the transmembrane region, and has been already functionalized with other heterologous domains for vaccination purposes in the context of recombinant rabies virions that display fusion proteins on their surface (Larson et al. 2006) as well as in the genome of the rabies vector (Hennrich et al. 2021). Hennrich et al.'s approach focused on fusing RBD of SARS-CoV-2 directly to RVG stem and anchoring regions, confirming its efficient incorporation in rabies and vesicular stomatitis virions. However, the co-expression of other viral proteins was necessary to incorporate the fusion protein in viral particles as it did not evidence autonomous budding activity.

Interestingly, using flow cytometry and laser confocal microscopy, we were able to demonstrate that S-RVG fusion

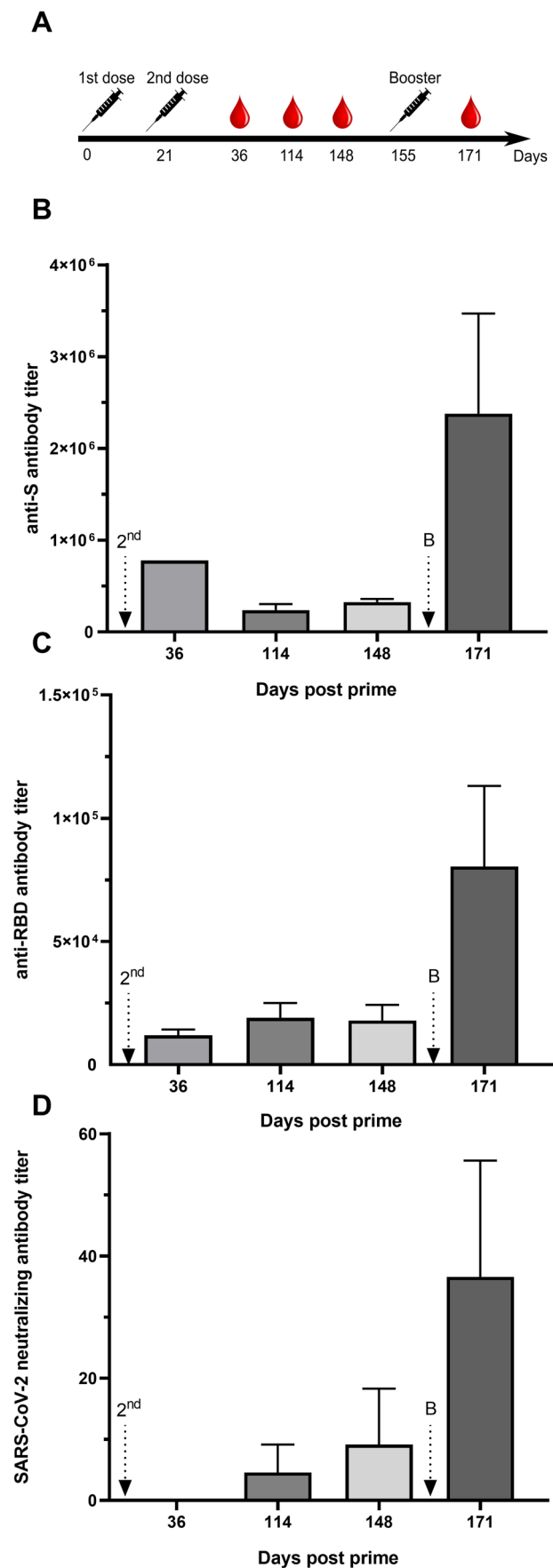
Fig. 7 Humoral immune response triggered by cVLPs. Balb/c mice were intramuscularly injected with a formulation containing SARS-CoV-2 cVLPs through a two-dose and booster immunization plan (A). Anti-S (B) and anti-RBD (C) antibodies were quantified by indirect ELISA and neutralizing antibodies (D) by a virus neutralization assay. For B and C, antibody titers were calculated as the highest dilution that gave a signal higher than the cutoff, which was established as the mean + 2SD of a negative serum. For D, titer was established as the highest dilution in which no cytopathic effect was observed in the culture. 2nd, second dose; B, booster. Bars indicate mean + SEM

protein was certainly detected on the surface of transfected HEK293 cells by a convalescent patient serum as well as by an anti-RBD mAb (Fig. 2 and Fig. 3), suggesting an adequate antigenic conformation. Furthermore, considering that the mAb is a neutralizing antibody, this recognition indicated that RBD displays the ACE2 recognition motif (receptor binding motif (Yi et al. 2020)) in the context of the fusion protein.

By western blot analysis, S-RVG fusion protein could be detected both in culture supernatants and in concentrated sucrose cushion ultracentrifugated samples (Fig. 4), suggesting its ability to autonomously bud forming enveloped cVLPs. This hypothesis was confirmed by TEM and gold-labeled immune TEM. Furthermore, we observed glycoprotein projections on the surface of the particles resembling a “corona-like” structure (Fig. 5A), similar to those observed on native SARS-CoV-2 virions. Besides, specific recognition of a SARS-CoV-2 neutralizing antibody confirmed a correct display of RBD in the context of the cVLP (Fig. 5B). Electron micrograph measures indicated that this cVLP has a similar size (76 ± 21 nm) to that of native SARS-CoV-2 virions, ranging from 70 to 100 nm (Menter et al. 2020) or 67 ± 15 nm (Varga et al. 2020).

Regarding the protein yield obtained, we could estimate a value of 48 μ g of S-RVG protein associated to cVLPs per liter of culture medium (data not shown). Unfortunately, it is difficult to compare this value with bibliographic data, since other SARS-CoV-2 VLP developments report their yield in terms of VLP mass or units per milliliter (Swann et al. 2020; Jaron et al. 2022). However, in terms of soluble S ectodomain production, our yield turns to be similar to those obtained for difficult to express S ectodomain sequences, which are reported to reach around 20 μ g per liter of culture (Stalls et al. 2022). We consider that our S-RVG protein yield is encouraging, taking into account that obtaining high yields of enveloped VLPs is a challenging task (Arista-Romero et al. 2021).

S-RVG was as effective as native S protein to interact with ACE2 receptor in the context of a lentiviral vector (Fig. 6(A)); this result gave further evidence that RBD adopts a natural conformation on the surface of S-RVG. Importantly, we could also confirm that S-RVG is able to



bind to ACE2 in the context of the cVLP in flow cytometry assays, since S-RVG cVLPs containing Gag-GFP as a reporter protein were able to bind to ACE2 receptor and to be internalized in a specific manner in ACE2 HEK293 expressing cells (Fig. 6(B)).

Finally, we could verify cVLP immunogenicity in an immunization plan in Balb/c mice. Specific anti-S and anti-RBD antibodies were detected after two doses, and for at least 130 days from the second dose. A booster given at 150 days was able to increase antibody levels which surpassed those obtained in the first blood extraction (day 36, Fig. 7A, B). Currently, it is known that to achieve a protective immunological state against COVID-19, it is necessary to administer booster doses, as protection decays over time (Loubet et al. 2021). In fact, several clinical studies have been carried out to confirm booster dose effectiveness as part of currently available vaccine immunization plans (Voysey et al. 2021; Hung and Poland 2021; Barda et al. 2021).

Besides the generation of anti-S and anti-RBD antibodies, we confirmed cVLP potential to induce neutralizing antibodies (Fig. 7C). This type of antibodies was more effectively detected after the booster dose, in accordance with the raise of anti-RBD antibodies. Further studies remain to be carried out to optimize the amount of cVLPs per dose in order to improve the immune response triggered with this vaccine candidate. Despite the fact that little mass of S-containing cVLPs was administered per dose (150 ng), the neutralizing antibody levels obtained were not far from those reported in mice for SARS-CoV-2 VLPs, which ranged from 1/300 for a chemically coupled RBD capsid VLP using 20 µg per dose (Rothen et al. 2022), to 1/1079 with a VSV-G/S fusion protein Gag containing VLPs using 5 µg per dose (Fluckiger et al. 2021).

Further studies remain to be fulfilled to optimize the production of this vaccine candidate. On the one hand, volumetric yield can be increased by using suspension growth-adapted HEK293 cells, which can be cultured to higher densities and efficiently transfected for the transient production of enveloped VLPs (Cervera et al. 2013; Venereo-Sanchez et al. 2016; Venereo-Sánchez et al. 2019; Lavado-García et al. 2020). In fact, we have previously tested this suspension expression platform with a cVLP containing a fusion rabies glycoprotein with good results (Fontana et al. 2021b). On the other hand, the use of recombinant stable expressing HEK293 cell lines represents an approach that can be also addressed to obtain high yield production of enveloped VLPs, as previous works with RVG VLPs and fusion RVG proteins have proven (Fontana et al. 2014; Fontana et al. 2015b; Fontana et al. 2019; Fontana et al. 2020; Garay et al. 2022). This strategy has been further optimized with RVG VLPs, using a suspension growth-adapted stable expressing clone in a 5-L bioreactor operated in perfusion

mode, achieving high productivity of enveloped VLPs (Fontana et al. 2015b).

As a conclusion, we designed and expressed a novel fusion protein that exposes S ectodomain in the context of RVG anchoring region. This construct expressed in HEK293 cells is able to bud forming SARS-CoV-2 cVLPs displaying S on their surface and resembling the structure of native SARS-CoV-2. Moreover, cVLPs are able to induce humoral responses and thus have the potential to become a novel vaccine candidate against COVID-19 that can be efficiently produced by expressing a single chimeric construction.

Author contribution EG and DF wrote the manuscript. EG, CP, and DF designed the fusion protein sequence. EG, JV, JMB, and VG constructed the expression plasmid. EG and JMB conducted protein expression analysis by flow cytometry and laser confocal microscopy. EG performed TEM cVLP analysis and lentiviral transduction assays. EG and JV performed western blot assays. EG, AF, and DF conducted the immunization protocol. EG, AF, AG, and NC extracted blood samples. JV, AF, SA, MCR, and BT produced and purified RBD and soluble S protein for indirect ELISA assays. DA, EC, and JC conducted neutralizing antibody determination assays. DF, CP, and NC revised the manuscript. All authors read and approved the manuscript.

Funding This work was supported by the Agencia Nacional de Promoción de la Investigación, el Desarrollo Productivo y la Innovación (Agencia I + D + i) (IP-COVID-19-224).

Data availability The data generated and analyzed in the present study is included in this published article.

Declarations

Ethics approval The immunization protocols were approved and supervised by the Advisory Committee on Ethics and Security of the School of Biochemistry and Biological Sciences, Universidad Nacional del Litoral, according to international guidelines (“Guide for the Care and Use of Laboratory Animals,” Eighth Edition National Research Council 2011).

Conflict of interest The authors declare no competing interests.

References

- Arista-Romero M, Delcanale P, Pujals S, Albertazzi L (2021) Nanoscale mapping of recombinant viral proteins: from cells to virus-like particles. *ACS Photonics* 9:101–109. <https://doi.org/10.1021/acsp Photonics.1c01154>
- Aston-Deaville S, Carlsson E, Saleem M, Thistlethwaite A, Chan H, Maharjan S, Facchetti A, Feavers IM, Alistair Siebert C, Collins RF, Roseman A, Derrick JP (2020) An assessment of the use of hepatitis B virus core protein virus-like particles to display heterologous antigens from *Neisseria meningitidis*. *Vaccine* 38:3201–3209. <https://doi.org/10.1016/j.vaccine.2020.03.001>
- Baden LR, El Sahly HM, Essink B, Kotloff K, Frey S, Novak R, Diemert D, Spector SA, Rouphael N, Creech CB, McGettigan J, Khetan S, Segall N, Solis J, Brosz A, Fierro C, Schwartz H, Neuzil K, Corey L et al (2021) Efficacy and safety of the mRNA-1273 SARS-CoV-2 vaccine. *N Engl J Med* 384:403–416. <https://doi.org/10.1056/NEJMoa210831>

- doi.org/10.1056/NEJMOA2035389/SUPPL_FILE/NEJMOA2035389_DATA-SHARING.PDF
- Barda N, Dagan N, Cohen C, Hernán MA, Lipsitch M, Kohane IS, Reis BY, Balicer RD (2021) Effectiveness of a third dose of the BNT162b2 mRNA COVID-19 vaccine for preventing severe outcomes in Israel: an observational study. *Lancet* 398:2093–2100. [https://doi.org/10.1016/S0140-6736\(21\)02249-2](https://doi.org/10.1016/S0140-6736(21)02249-2)
- Battagliotti JM, Fontana D, Etcheverrigaray M, Kratje R, Prieto C (2020) Characterization of hepatitis B virus surface antigen particles expressed in stably transformed mammalian cell lines containing the large, middle and small surface protein. *Antiviral Res* 183:104936. <https://doi.org/10.1016/j.antiviral.2020.104936>
- Bertona D, Pujato N, Bontempi I, Gonzalez V, Cabrera G, Gugliotta L, Hozbor D, Nicastro A, Calvino L, Marcipar IS (2017) Development and assessment of a new cage-like particle adjuvant. *J Pharm Pharmacol* 69(10):1293–1303. <https://doi.org/10.1111/jphp.12768>
- Bidart J, Kornuta C, Gammella M, Gnazzo V, Soria I, Langellotti C, Mongini C, Galarza R, Calvino L, Lupi G, Quattrocchi V, Marcipar I, Zamorano P (2020) A new cage-like particle adjuvant enhances protection of foot-and-mouth disease vaccine. *Front Vet Sci* 7:1–12. <https://doi.org/10.3389/fvets.2020.00396>
- Bidart J, Mignaqui A, Kornuta C, Lupi G, Gammella M, Soria I, Galarza R, Ferella A, Cardillo S, Langellotti C, Quattrocchi V, Durocher Y, Wigdorovitz A, Marcipar I, Zamorano P (2021) FMD empty capsids combined with the immunostimulant particle adjuvant -ISPA or ISA206 induce protective immunity against foot and mouth disease virus. *Virus Res* 297:198339. <https://doi.org/10.1016/j.virusres.2021.198339>
- Callaway HM, Zyla D, Larrous F, de Melo GD, Hastie KM, Avalos RD, Agarwal A, Corti D, Bourhy H, Saphire EO (2022) Structure of the rabies virus glycoprotein trimer bound to a prefusion-specific neutralizing antibody. *Sci Adv* 8:eabp9151. <https://doi.org/10.1126/sciadv.abp9151>
- Cervera L, Gutiérrez-Granados S, Martínez M, Blanco J, Gòdia F, Segura MM (2013) Generation of HIV-1 Gag VLPs by transient transfection of HEK 293 suspension cell cultures using an optimized animal-derived component free medium. *J Biotechnol* 166:152–165. <https://doi.org/10.1016/j.jbiotec.2013.05.001>
- Coria LM, Saposnik LM, Pueblas Castro C, Castro EF, Bruno LA, Stone WB, Pérez PS, Darriba ML, Chemes LB, Alcain J, Mazzitelli I, Varese A, Salvatori M, Auguste AJ, Álvarez DE, Pasquevich KA, Cassataro J (2022) A novel bacterial protease inhibitor adjuvant in RBD-based COVID-19 vaccine formulations containing alum increases neutralizing antibodies, specific germinal center B cells and confers protection against SARS-CoV-2 infection in mice. *Front Immunol* 13:604. <https://doi.org/10.3389/FIMMU.2022.844837/BIBTEX>
- Crawford KHD, Eguia R, Dingens AS, Loes AN, Malone KD, Wolf CR, Chu HY, Tortorici MA, Veelsler D, Murphy M, Pettie D, King NP, Balazs AB, Bloom JD (2020) Protocol and reagents for pseudotyping lentiviral particles with SARS-CoV-2 spike protein for neutralization assays. *Viruses* 12:513. <https://doi.org/10.3390/V12050513>
- Cutler DM, Summers LH (2020) The COVID-19 pandemic and the \$16 trillion virus. *JAMA* 324:1495–1496. <https://doi.org/10.1001/JAMA.2020.19759>
- Czarnota A, Anna O, Pihl AF, Prentoe J (2020) Specific antibodies induced by immunization with hepatitis B virus-like particles carrying hepatitis C virus envelope glycoprotein 2 epitopes show differential neutralization e ffi ciency. *Vaccine* 8:1–19. <https://doi.org/10.3390/vaccines8020294>
- del Carmen M-GA, Rivera-Toledo E, Echeverría O, Vázquez-Nin G, Gómez B, Bustos-Jaimes I (2016) Peptide presentation on primate erythrovirus 1 virus-like particles: in vitro assembly, stability and immunological properties. *Virus Res* 224:12–18. <https://doi.org/10.1016/j.virusres.2016.08.007>
- Donaldson B, Lateef Z, Walker GF, Young SL, Ward VK (2018) Virus-like particle vaccines: immunology and formulation for clinical translation. *Expert Rev Vaccines* 17:833–849. <https://doi.org/10.1080/14760584.2018.1516552>
- Etzion O, Novack V, Perl Y, Abel O, Schwartz D, Munteanu D, Abufreha N, Ben-Yaakov G, Maoz ED, Moshaklo A, Dizingf V, Fich A (2016) Sci-B-VacTM Vs ENGERIX-B vaccines for hepatitis B virus in patients with inflammatory bowel diseases: a randomised controlled trial. *J Crohns Colitis* 10:905. <https://doi.org/10.1093/ECCO-JCC/JJW046>
- Fluckiger AC, Ontsouka B, Bozic J, Diress A, Ahmed T, Berthoud T, Tran A, Duque D, Liao M, McCluskie M, Diaz-Mitoma F, Anderson DE, Soare C (2021) An enveloped virus-like particle vaccine expressing a stabilized prefusion form of the SARS-CoV-2 spike protein elicits highly potent immunity. *Vaccine* 39:4988–5001. <https://doi.org/10.1016/J.VACCINE.2021.07.034>
- Fontana D, Kratje R, Etcheverrigaray M, Prieto C (2014) Rabies virus-like particles expressed in HEK293 cells. *Vaccine* 32:2799–2804. <https://doi.org/10.1016/j.vaccine.2014.02.031>
- Fontana D, Kratje R, Etcheverrigaray M, Prieto C (2015a) Immunogenic virus-like particles continuously expressed in mammalian cells as a veterinary rabies vaccine candidate. *Vaccine* 33:4238–4246. <https://doi.org/10.1016/j.vaccine.2015.03.088>
- Fontana D, Kratje R, Etcheverrigaray M, Prieto C (2015b) Immunogenic virus-like particles continuously expressed in mammalian cells as a veterinary rabies vaccine candidate. *Vaccine* 33:4238–4246. <https://doi.org/10.1016/J.VACCINE.2015.03.088>
- Fontana D, Etcheverrigaray M, Kratje R, Prieto C (2016) Development of rabies virus-like particles for vaccine applications: production, characterization, and protection studies. *Methods Mol Biol* 1403:155–166. https://doi.org/10.1007/978-1-4939-3387-7_7
- Fontana D, Marsili F, Garay E, Battagliotti J, Etcheverrigaray M, Kratje R, Prieto C (2019) A simplified roller bottle platform for the production of a new generation VLPs rabies vaccine for veterinary applications. *Comp Immunol Microbiol Infect Dis* 65:70–75. <https://doi.org/10.1016/j.cimid.2019.04.009>
- Fontana D, Marsili F, Etcheverrigaray M, Kratje R, Prieto C (2020) Rabies VLPs adjuvanted with saponin-based liposomes induce enhanced immunogenicity mediated by neutralizing antibodies in cattle, dogs and cats. *J Virol Methods* 286:113966. <https://doi.org/10.1016/j.jviromet.2020.113966>
- Fontana D, Garay E, Cervera L, Kratje R, Prieto C (2021a) Chimeric VLPs based on HIV-1 Gag and a fusion rabies glycoprotein induce specific antibodies against rabies and foot-and-mouth disease virus. *Vaccines* 9(3):251. <https://doi.org/10.3390/vaccines9030251>
- Fontana D, Garay E, Cervera L, Kratje R, Prieto C, Gòdia F (2021b) Chimeric vlpS based on hiv-1 gag and a fusion rabies glycoprotein induce specific antibodies against rabies and foot-and-mouth disease virus. *Vaccines* 9:251. <https://doi.org/10.3390/vaccines9030251>
- Garay E, Fontana D, Leschiutta L, Kratje R, Prieto C (2022) Rational design of novel fusion rabies glycoproteins displaying a major antigenic site of foot-and-mouth disease virus for vaccine applications. *Appl Microbiol Biotechnol* 106:579–592. <https://doi.org/10.1007/s00253-021-11747-4>
- Garçon N, Vaughn DW, Didierlaurent AM (2012) Development and evaluation of AS03, an adjuvant system containing α -tocopherol and squalene in an oil-in-water emulsion. *Expert Rev Vaccines* 11:349–366. <https://doi.org/10.1586/ERV.11.192>
- Gutiérrez-Granados S, Cervera L, Gòdia F, Segura MM (2013) Characterization and quantitation of fluorescent Gag virus-like particles. *BMC Proc* 7:P62. <https://doi.org/10.1186/1753-6561-7-S6-P62>
- Hager KJ, Marc GP, Gobeil P, Diaz RS, Heizer G, Llapur C, Makarkov AI, Vasconcellos E, Pillet S, Riera F, Saxena P, Wolff PG, Bhutata

- K, Wallace G, Aazami H, Jones CE, Polack FP, Ferrara L, Atkins J et al (2022) Efficacy and safety of a recombinant plant-based adjuvanted Covid-19 vaccine. *N Engl J Med* 386:2084–2096. <https://doi.org/10.1056/NEJMOA2201300>
- Heath PT, Galiza EP, Baxter DN, Boffito M, Browne D, Burns F, Chadwick DR, Clark R, Cosgrove C, Galloway J, Goodman AL, Heer A, Higham A, Iyengar S, Jamal A, Jeanes C, Kalra PA, Kyriakidou C, McAuley DF et al (2021) Safety and efficacy of NVX-CoV2373 Covid-19 vaccine. *N Engl J Med* 385:1172–1183. https://doi.org/10.1056/NEJMOA2107659/SUPPL_FILE/NEJMOA2107659_DATA-SHARING.PDF
- Henrich AA, Sawatsky B, Santos-Mandujano R, Banda DH, Oberhuber M, Schopf A, Pfaffinger V, Wittwer K, Riedel C, Pfaller CK, Conzelmann KK (2021) Safe and effective two-in-one replicon-and-VLP minispike vaccine for COVID-19: protection of mice after a single immunization. *PLoS Pathog* 17:1–25. <https://doi.org/10.1371/journal.ppat.1009064>
- Hung IFN, Poland GA (2021) Single-dose Oxford–AstraZeneca COVID-19 vaccine followed by a 12-week booster. *Lancet* 397:854. [https://doi.org/10.1016/S0140-6736\(21\)00528-6](https://doi.org/10.1016/S0140-6736(21)00528-6)
- Jaron M, Lehky M, Zarà M, Zaydowicz CN, Lak A, Ballmann R, Heine PA, Wenzel EV, Schneider KT, Bertoglio F, Kempter S, Köster RW, Barbieri SS, van den Heuvel J, Hust M, Dübel S, Schubert M (2022) Baculovirus-Free SARS-CoV-2 virus-like particle production in insect cells for rapid neutralization assessment. *Viruses* 14:2087. <https://doi.org/10.3390/V14102087/S1>
- Larson ME, Sherman MA, Greimel S, Kuskowski M, Schneider A, Bennett DA, Lesné SE (2006) Rabies virus glycoprotein as a carrier for anthrax protective antigen. *Virology* 32:10253–10266. <https://doi.org/10.1523/JNEUROSCI.0581-12.2012.Soluble>
- Laurens MB (2020) RTS,S/AS01 vaccine (Mosquirix™): an overview. *Hum Vaccin Immunother* 16:480. <https://doi.org/10.1080/21645515.2019.1669415>
- Lavado-García J, Cervera L, Gòdia F (2020) An alternative perfusion approach for the intensification of virus-like particle production in HEK293 cultures. *Front Bioeng Biotechnol* 8:617. <https://doi.org/10.3389/FBIOE.2020.00617>
- Liu X, Fang Y, Zhou P, Lu Y, Zhang Q, Xiao S, Dong Z, Pan L, Lv J, Zhang Z, Zhang Y, Wang Y (2017) Chimeric virus-like particles elicit protective immunity against serotype O foot-and-mouth disease virus in guinea pigs. *Appl Microbiol Biotechnol* 101(12):4905–4914. <https://doi.org/10.1007/s00253-017-8246-0>
- Loubet P, Laureillard D, Martin A, Larcher R, Sotto A (2021) Why promoting a COVID-19 vaccine booster dose? *Anaesth Crit Care Pain Med* 40:100967. <https://doi.org/10.1016/J.ACCPM.2021.100967>
- Lua LHL, Connors NK, Sainsbury F, Chuan YP, Wibowo N, Middeberg APJ (2014) Bioengineering virus-like particles as vaccines. *Biotechnol Bioeng* 111:425–440. <https://doi.org/10.1002/bit.25159>
- Mareze VA, Borio CS, Bilén MF, Fleith R, Mirazo S, Mansur DS, Arbiza J, Lozano ME, Bruña-Romero O (2016) Tests in mice of a dengue vaccine candidate made of chimeric Junin virus-like particles and conserved dengue virus envelope sequences. *Appl Microbiol Biotechnol* 100:125–133. <https://doi.org/10.1007/s00253-015-6973-7>
- Menter T, Haslbauer JD, Nienhold R, Savic S, Hopfer H, Deigendesch N, Frank S, Turek D, Willi N, Pargger H, Bassetti S, Leuppi JD, Cathomas G, Tolnay M, Mertz KD, Tzankov A (2020) Postmortem examination of COVID-19 patients reveals diffuse alveolar damage with severe capillary congestion and variegated findings in lungs and other organs suggesting vascular dysfunction. *Histopathology* 77:198–209. <https://doi.org/10.1111/HIS.14134>
- Mohsen MO, Zha L, Cabral-Miranda G, Bachmann MF (2017) Major findings and recent advances in virus-like particle (VLP)-based vaccines. *Semin Immunol* 34:123–132. <https://doi.org/10.1016/j.smim.2017.08.014>
- Polack FP, Thomas SJ, Kitchin N, Absalon J, Gurtman A, Lockhart S, Perez JL, Pérez Marc G, Moreira ED, Zerbini C, Bailey R, Swanson KA, Roychoudhury S, Koury K, Li P, Kalina WV, Cooper D, Frenck RW, Hammitt LL et al (2020) Safety and efficacy of the BNT162b2 mRNA Covid-19 vaccine. *N Engl J Med* 383:2603–2615. https://doi.org/10.1056/NEJMOA2034577/SUPPL_FILE/NEJMOA2034577_PROTOCOL.PDF
- Prieto C, Fontana D, Etcheverrigaray M, Kratje R (2011) A strategy to obtain recombinant cell lines with high expression levels. *Lentiviral vector-mediated transgenesis. BMC Proc* 5(Suppl 8):P7. <https://doi.org/10.1186/1753-6561-5-S8-P7>
- Rothen DA, Krenger PS, Nonic A, Balke I, Vogt ACS, Chang X, Manenti A, Vedovi F, Resevica G, Walton SM, Zeltins A, Montomoli E, Vogel M, Bachmann MF, Mohsen MO (2022) Intranasal administration of a VLP-based vaccine induces neutralizing antibodies against SARS-CoV-2 and variants of concern. *Allergy* 77:2446–2458. <https://doi.org/10.1111/ALL.15311>
- Sadoff J, Le Gars M, Shukarev G, Heerwegh D, Truyers C, de Groot AM, Stoop J, Tete S, Van Damme W, Leroux-Roels I, Berghmans P-J, Kimmel M, Van Damme P, de Hoon J, Smith W, Stephenson KE, De Rosa SC, Cohen KW, McElrath MJ et al (2021) Interim results of a phase 1–2a trial of Ad26.COV2.S Covid-19 vaccine. *N Engl J Med* 384:1824–1835. https://doi.org/10.1056/NEJMOA2034201/SUPPL_FILE/NEJMOA2034201_DATA-SHARING.PDF
- Schiller JT, Castellsagué X, Garland SM (2012) A review of clinical trials of human papillomavirus prophylactic vaccines. *Vaccine* 30:F123. <https://doi.org/10.1016/J.VACCINE.2012.04.108>
- Schindelin J, Arganda-Carreras I, Frise E, Kaynig V, Longair M, Pietzsch T, Preibisch S, Rueden C, Saalfeld S, Schmid B, Tinevez JY, White DJ, Hartenstein V, Eliceiri K, Tomancak P, Cardona A (2012) Fiji: an open-source platform for biological-image analysis. *Nat Methods* 9:676–682. <https://doi.org/10.1038/nmeth.2019>
- Stalls V, Janowska K, Acharya P (2022) Transient transfection and purification of SARS-CoV-2 spike protein from mammalian cells. *STAR Protoc* 3:101603. <https://doi.org/10.1016/J.XPRO.2022.101603>
- Swann H, Sharma A, Preece B, Peterson A, Eldridge C, Belnap DM, Vershinin M (2020) Saffarian S (2020) Minimal system for assembly of SARS-CoV-2 virus like particles. *Sci Rep* 10(10):1–5. <https://doi.org/10.1038/s41598-020-78656-w>
- Tai W, He L, Zhang X, Pu J, Voronin D, Jiang S, Zhou Y, Du L (2020) Characterization of the receptor-binding domain (RBD) of 2019 novel coronavirus: implication for development of RBD protein as a viral attachment inhibitor and vaccine. *Cell Mol Immunol* 17(6):613–620. <https://doi.org/10.1038/s41423-020-0400-4>
- Tanriover MD, Doğanay HL, Akova M, Güner HR, Azap A, Akhan S, Köse Ş, Erdiñç FŞ, Akalın EH, Tabak ÖF, Pullukçu H, Batum Ö, Şimşek Yavuz S, Turhan Ö, Yıldırım MT, Köksal İ, Taşova Y, Korten V, Yılmaz G et al (2021) Efficacy and safety of an inactivated whole-virion SARS-CoV-2 vaccine (CoronaVac): interim results of a double-blind, randomised, placebo-controlled, phase 3 trial in Turkey. *Lancet (London, England)* 398:213–222. [https://doi.org/10.1016/S0140-6736\(21\)01429-X](https://doi.org/10.1016/S0140-6736(21)01429-X)
- Varga Z, Flammer AJ, Steiger P, Haberecker M, Andermatt R, Zinkernagel A, Mehra MR, Scholkmann F, Schüpbach R, Ruschitzka F, Moch H (2020) Electron microscopy of SARS-CoV-2: a challenging task – Authors’ reply. *Lancet* 395:e100. [https://doi.org/10.1016/S0140-6736\(20\)31185-5](https://doi.org/10.1016/S0140-6736(20)31185-5)
- Venereo-Sanchez A, Gilbert R, Simoneau M, Caron A, Chahal P, Chen W, Ansoorge S, Li X, Henry O, Kamen A (2016) Hemagglutinin and neuraminidase containing virus-like particles produced in HEK-293 suspension culture: an effective influenza vaccine candidate. *Vaccine* 34:3371–3380. <https://doi.org/10.1016/j.vaccine.2016.04.089>

- Venereo-Sánchez A, Fulton K, Koczka K, Twine S, Chahal P, Ansoorge S, Gilbert R, Henry O, Kamen A (2019) Characterization of influenza H1N1 Gag virus-like particles and extracellular vesicles co-produced in HEK-293SF. *Vaccine* 37:7100–7107. <https://doi.org/10.1016/j.vaccine.2019.07.057>
- Voysey M, Clemens SAC, Madhi SA, Weckx LY, Folegatti PM, Aley PK, Angus B, Baillie VL, Barnabas SL, Bhorat QE, Bibi S, Briner C, Cicconi P, Collins AM, Colin-Jones R, Cutland CL, Darton TC, Dheda K, Duncan CJA et al (2021) Safety and efficacy of the ChAdOx1 nCoV-19 vaccine (AZD1222) against SARS-CoV-2: an interim analysis of four randomised controlled trials in Brazil, South Africa, and the UK. *Lancet* 397:99–111. [https://doi.org/10.1016/S0140-6736\(20\)32661-1](https://doi.org/10.1016/S0140-6736(20)32661-1)
- Walls AC, Park Y, Tortorici MA, Wall A, McGuire AT, Veerler D (2020) Structure, function, and antigenicity of the SARS-CoV-2 spike glycoprotein. *Cell* 180:281–292
- Watson OJ, Barnsley G, Toor J, Hogan AB, Winskill P, Ghani AC (2022) Global impact of the first year of COVID-19 vaccination: a mathematical modelling study. *Lancet Infect Dis* 22(9):1293–1302. [https://doi.org/10.1016/s1473-3099\(22\)00320-6](https://doi.org/10.1016/s1473-3099(22)00320-6)
- Xia S, Zhang Y, Wang Y, Wang H, Yang Y, Gao GF, Tan W, Wu G, Xu M, Lou Z, Huang W, Xu W, Huang B, Wang H, Wang W, Zhang W, Li N, Xie Z, Ding L et al (2021) Safety and immunogenicity of an inactivated SARS-CoV-2 vaccine, BBIBP-CorV: a randomised, double-blind, placebo-controlled, phase 1/2 trial. *Lancet Infect Dis* 21:39–51. [https://doi.org/10.1016/S1473-3099\(20\)30831-8](https://doi.org/10.1016/S1473-3099(20)30831-8)
- Xu L, He D, Yang L, Li Z, Ye X, Yu H, Zhao H, Li S, Yuan L, Qian H, Que Y, Kuo Shih JW, Zhu H, Li Y, Cheng T, Xia N (2015) A broadly cross-protective vaccine presenting the neighboring epitopes within the VP1 GH loop and VP2 EF loop of Enterovirus 71. *Sci Rep* 5:12973. <https://doi.org/10.1038/srep12973>
- Xu R, Shi M, Li J, Song P, Li N (2020) Construction of SARS-CoV-2 virus-like particles by mammalian expression system. *Front Bioeng Biotechnol* 8:862. <https://doi.org/10.3389/fbioe.2020.00862>
- Yi C, Sun X, Ye J, Ding L, Liu M, Yang Z, Lu X, Zhang Y, Ma L, Gu W, Qu A, Xu J, Shi Z, Ling Z (2020) Sun B (2020) Key residues of the receptor binding motif in the spike protein of SARS-CoV-2 that interact with ACE2 and neutralizing antibodies. *Cell Mol Immunol* 176(17):621–630. <https://doi.org/10.1038/s41423-020-0458-z>

Publisher's note Springer Nature remains neutral with regard to jurisdictional claims in published maps and institutional affiliations.

Springer Nature or its licensor (e.g. a society or other partner) holds exclusive rights to this article under a publishing agreement with the author(s) or other rightsholder(s); author self-archiving of the accepted manuscript version of this article is solely governed by the terms of such publishing agreement and applicable law.